Magnetic Magnetite/Epoxy Nanocomposites with Polyaniline as Coupling Agent: Preparation, Characterization and Property

Juanna Ren
Taiyuan University of Science and Technology
Wenhao Dong
Taiyuan University of Science and Technology
Ethan Burcar
Oakland University
Ashley DeMerle
Oakland University
Zhe Wang
zhewang@oakland.edu
Oakland University
Hua Hou
Taiyuan University of Science and Technology

Research Article

Keywords: Polyaniline@magnetite, Epoxy Nanocomposites, Electromagnetic Wave Adsorption

Posted Date: December 13th, 2024

DOI: https://doi.org/10.21203/rs.3.rs-5120342/v1

Additional Declarations: No competing interests reported.

Version of Record: A version of this preprint was published at Advanced Composites and Hybrid Materials on December 27th, 2024. See the published version at https://doi.org/10.1007/s42114-024-01166-0.

Abstract

An in-situ polymerization method fabricated the electrically conductive magnetic epoxy nanocomposites with polyaniline@magnetite. With the introduction of polyaniline on the magnetite nanoparticles, the structural integrity of the synthesized epoxy nanocomposites was enhanced with the bridging effect of the polyaniline. Specifically, compared with pure epoxy, the tensile strength was improved to 82.2 MPa when 1.0 wt% polyaniline@magnetite was added to the epoxy matrix. The enhanced mechanical property is due to the enhanced interfacial interaction. With further increasing particle loading to 30.0 wt%, glass transition temperature (T_g) was decreased to 85.4 ^oC, which is related to the enlarged free volume between epoxy chains. The saturation magnetization of 30.0 wt% polyaniline@magnetite-epoxy composites was 12.79 emu/g. Moreover, with the assistance of polyaniline@magnetite, the thermal stability was enhanced compared with pure epoxy. The electromagnetic wave absorption of the unique polyaniline@magnetite/epoxy nanocomposites was also studied. When the content of polyaniline@magnetite reached 30.0 wt%, the reflection loss even reached 35.9 dB. This work guides the fabrication of multifunctional epoxy nanocomposites with comprehensive electrical, magnetic and mechanical properties.

1. Introduction

As one of the most popular engineered thermosetting materials, epoxy is applied in different fields, including anticorrosion, adhesives, and electronics encapsulation materials, due to its excellent mechanical properties and chemical stability [1–3]. In order to widen its application in new areas, researchers have done many works by adding different fillers with different functions into thermosetting epoxy [4–7]. For instance, Gu *et al.* added SiO_2 into the epoxy matrix to enhance the mechanical properties of epoxy nanocomposites [8]. Gu *et al.* successfully enhanced the mechanical and electrical properties by adding carbon nanofillers with various dimensions into the epoxy matrix [9]. Both mechanical and electrical properties were enhanced at the same time with a relatively low nanocarbons loading. However, the agglomeration of the nanoparticles would appear with high nanofiller loadings.

The surface treatment of the nanofillers has attracted the attention of researchers to overcome the above aggregation issue. There are two main methods of surface treatment. On the one hand, the nanofillers are directly treated by chemicals to introduce functional groups. For example, Gu *et al.* treated the carbon nanofibers with concentrated acid to introduce carboxyl functional groups on the carbon nanofibers, which could react with epoxide groups [9]. The electrical and mechanical properties are improved. On the other hand, a coupling agent such as silane is applied to form a chemical bond bridge between the nanofiller and polymer matrix. For instance, Zhang *et al.* applied KH550 on the surface of ZnO to overcome the agglomeration [10]. And the mechanical property is significantly improved.

Due to its relatively high saturation magnetization, magnetite (Fe_3O_4) has been applied for catalysis, information storage, color imaging, etc [11–14]. Fe_3O_4 in the epoxy matrix could widen its applications in

electronic, energy storage, and environment remediation [12, 15–18]. To overcome the agglomeration of Fe_3O_4 nanoparticles, coupling agents such as saline have been applied to do the surface treatment of the Fe_3O_4 nanoparticles. Among the conjugated conductive polymers, polyaniline (PANI) has attracted more attention from researchers and has been applied in various ways due to its unique chemical structure, tunable electrical properties, etc. For example, Guo *et al.* reported the enhanced mechanical and electrical properties of the polyaniline/epoxy nanocomposites due to the formed chemical bond between epoxy and polyaniline fillers [19]. However, there is less work evaluating the effect of polyaniline as the coupling agent on mechanical properties, thermal stability, electromagnetic properties and magnetic properties in the magnetic epoxy nanocomposites with magnetite nanoparticles as fillers.

In this work, PANI@Fe_3O_4/epoxy nanocomposites were prepared using the situ polymerization method. The chemical and crystal structure and morphology of PANI@Fe_3O_4 nanoparticles are characterized by Fourier transform infrared spectroscopy, scanning electron microscopy and X-ray diffractometer. The roles of PANI coating on thermal stability, mechanical properties, and magnetic properties were studied. FTIR and a differential scanning calorimeter analyzed the chemical bond formation mechanism. Moreover, the electromagnetic wave absorbing property of the PANI@Fe_3O_4/epoxy nanocomposites was evaluated as well.

2. Experimentals

2.1 Materials

The PANI@Fe_3O_4 nanoparticles were bought from Chongqing Huancai Materials Technology Co., Ltd., Chongqing, China. The epon monomers (EPON 862) were all brought from Guangzhou Diexun Trading Co., Ltd., China. The curing agent (EpiCure W) was brought from Guangzhou Diexun Trading Co., Ltd., China. The details about the preparation of PANI@Fe_3O_4/epoxy nanocomposites and characterization are in the supporting materials.

3. Results and Discussion

Morphology, chemical structure and crystal structure are analyzed by SEM, FT-IR and XRD as shown in Fig. 1. The PANI@Fe_3O_4 particles are spheres with a diameter of about 110 nm, obtained through nanomeasurer software as shown in Fig. 1(a). The peaks at 1578, 1493, 1300, 1226, 1118, 803, 628 and 580 cm^{-1} observed in the FT-IR reflect the characteristic peak of pure PANI [11], as shown in Fig. 1(b). Meanwhile, the crystal peaks located at 30, 35, 43, 54, 58, and 62^o indicate the crystal phase of (220), (311), (400), (422), (511) and (400) of Fe_3O_4 particles [11, 20]. The SEM, FT-IR and XRD results show that the polyaniline is well coated on Fe_3O_4 nanoparticles, indicating the core-shell structure of PANI@Fe_3O_4 particles.

Figure 2(A) shows stress-strain curves for epoxy nanocomposites with varying loadings of PANI@Fe_3O_4 nanoparticles. The pure epoxy's tensile strength is 78.8 MPa. For epoxy nanocomposites, the tensile strength is improved to be 82.2 MPa even when the PANI@Fe_3O_4 nanoparticles is low (1.0 wt%). The improved tensile strength is attributed to the polyaniline functionalized Fe_3O_4, which enhances the interfacial reaction between Fe_3O_4 and epoxy. With further increasing the PANI@Fe_3O_4 nanoparticles loading to 10.0 and 30.0 wt%, tensile strength is decreased to 62.3 and 35.6 MPa, respectively. The decreased tensile strength is due to the agglomeration of PANI@Fe_3O_4. The Young's modulus of pure epoxy and epoxy nanocomposites with 1.0, 10.0 and 30.0 wt% PANI@Fe_3O_4 particles is 1.22, 1.32, 1.41 and 1.40 GPa, respectively. Compared with pure epoxy, Young's modulus of epoxy nanocomposites is improved. With the introduction of PANI@Fe3O4 nanoparticles, the formed interfacial layer prevents the polymer's deformation, leading to an improved Young's modulus.

Figure. 3 displays SEM of the fracture surface of all samples after the tensile test. For pure epoxy, as shown in Fig. 3(a), a "river-like" fracture surface is observed, which indicates a brittle failure [19]. When the content of PANI@Fe_3O_4 nanoparticles is only 1.0 wt%, the epoxy nanocomposites also show a river-like fracture surface, Fig. 3(b). However, with further increasing the particle loading, agglomeration of PANI@Fe_3O_4 particles in epoxy is observed as shown in Fig. 3(c&d). When loading of PANI@Fe_3O_4 is 30.0 wt%, Fig. 3(d), agglomeration is obviously observed as marked by red cycle, leading to a decrease of tensile strength. A similar phenomenon is observed in PANI/epoxy nanocomposites [19].

Dynamic mechanical analysis (DMA) provides information on the storage modulus (G'), loss modulus (G"), and loss factor (tanδ) of pure epoxy and epoxy nanocomposites with different loadings of Fe_3O_4@PANI from 30 to 200 ^oC as shown in Fig. 4. Figure 4 demonstrates the dynamic mechanical analysis (DMA) results from 30 to 200 ^oC. The storage modulus (G') and loss modulus (G") are related to elastic property and energy dissipation of epoxy composites during the test, respectively. At glass state, Fig. 4(A), the G' of pure epoxy is about 3.4 GPa, and the G' for epoxy with 1.0, 10.0 and 30.0 wt% is 3.2, 3.8 and 5.9 GPa, respectively. The epoxy nanocomposites show higher G' than pure epoxy due to the confinement of polymer chains [21]. The epoxy nanocomposites with Fe@FeO and polypyrrole functionalized Fe_3O_4 nanoparticles also display similar results [21, 22]. Figure. 4(B) shows G" as a function of temperature from 30 to 200 ^oC for all samples. It is observed that G" shows a similar trend to G'. Generally, tan δ is the ratio of storage modulus to loss modulus, and the peak of tan δ is used to analyze glass transition temperature (T_g). Figure 4 (C) shows that the T_g of pure epoxy and epoxy nanocomposites with 1.0, 10.0 and 30.0 wt% is 128.3, 130.6, 123.1 and 85.4 ^oC, respectively. The introduction of PANI@Fe_3O_4 nanoparticles leads to decreasing Tg, due to enlarged free volume [23]. Similar results are also observed in graphene/epoxy nanocomposites [23].

Figure 5 displays room-temperature magnetization hysteresis curves of Fe_3O_4@PANI and its epoxy nanocomposites. As shown in Fig. 5(A), there is no hysteresis loop in the Fe_3O_4@PANI nanoparticles, demonstrating the superparamagnetic performance. However, a hysteresis loop is observed in the

Fe_3O_4@PANI-epoxy nanocomposites, Fig. 5(B). Generally, when coercivity (Hc) is larger than 200 Oe, the magnetic materials are defined as ferromagnetically hard. When the Hc is smaller than 200 Oe, the magnetic materials are defined as ferromagnetically soft. For all the Fe_3O_4@PANI-epoxy nanocomposites, Fig. 5(C), the Hc is smaller than 200 Oe. Hence, the Fe_3O_4@PANI-epoxy nanocomposites are ferromagnetically soft materials. It is obviously observed that the magnetization did not reach saturation in the measurement magnetic strength range. The saturation magnetization (Ms) can be determined by the extrapolated saturation magnetization obtained from the intercept of $M–H^{-1}$ at high fields. Obtained saturation magnetization is 40.30, 0.07, 3.77 and 12.79 emu/g for pure epoxy and epoxy nanocomposites with 1%, 10% and 30% Fe_3O_4@PANI nanoparticles, respectively.

Thermal stability is very important for the deployment of polymer nanocomposites. Figure 6 shows TGA and DTG results of all samples. For Fe_3O_4@PANI nanoparticles, Fig. 6(A), the final weight residue is about 82.8% at 800 ^oC. The weight loss is due to the degradation of polyaniline on the surface of Fe_3O_4. For pure epoxy, there are two major weight loss stages. The slight weight loss from 200 to 320 ^oC is due to the hemolytic scission of chemical bonds. The first weight loss from 350 to 450 ^oC is induced by the elimination of water molecules from the oxypropylene group, –CH2–CH(OH)–, and the simultaneous breakdown of the epoxy network [24]. With further increasing temperature, the second weight loss in the temperature range from 465 to 605 ^oC is due to degradation of benzene rings. For epoxy nanocomposites, two weight loss stages were observed. Compared with pure epoxy, the thermal stability of the epoxy nanocomposites is decreased, which is related to the obstructive effect of Fe_3O_4@PANI nanoparticles on the formation of high cross-linked molecular structure of epoxy matrix or the increased free volume fractions. Similar results are also observed in epoxy nanocomposites with different loadings of Fe@FeO [21]. Interestingly, the temperature at 50% weight loss of epoxy nanocomposites with 10 wt% and 30 wt% Fe_3O_4@PANI nanoparticles is higher than pure epoxy.

Electromagnetic parameters (ε', ε", μ', and μ") of Fe_3O_4@PANI nanoparticles/epoxy nanocomposites with 1.0, 10.0 and 30.0 wt% are displayed in Fig. 7(A, B, C). The positive dielectric constant is observed in all Fe_3O_4@PANI-epoxy composites, induced by the interfacial polarization formed at the interface between Fe_3O_4@PANI nanoparticles and epoxy matrix. The epoxy resin hindered the charge carriers, resulting in the accumulation of space charge carriers at the interface.

With increasing Fe_3O_4@PANI loading, the ε' and ε" increase. The μ' and μ" of the Fe_3O_4@PANI-epoxy composites is about 1 and 0. The reflection loss (RL) can be expressed as Eq. 1 [25, 26]:

$$\mathrm{RL} = 20 \log \left| \frac{Z_{in} - Z_0}{Z_{in} + Z_0} \right|$$

1

where Z_{in} and Z_0 represent input impedance and impedance in free space. Z_{in} and Z_0 are defined as Eqs. 2 and 3 [27]:

$$Z_{in} = \mathrm{Z}_0\sqrt{\frac{\mu_r}{\epsilon_r}}\tanh\left(j\frac{2\pi\, df\sqrt{\mu_r\epsilon_r}}{c}\right)$$

2

$$Z_0 = \sqrt{\frac{\mu_0}{\epsilon_0}}$$

3

where ε_r and μ_r are complex relative permittivity and complex relative permeability, d is the thickness of the material, c stands for velocity of EM wave in vacuum and f stands for the frequency of EM wave. Figure 7 displays reflection loss as a function of frequency from 2 to 18 GHz of the epoxy nanocomposites. For epoxy nanocomposites with 1.0 wt% Fe_3O_4@PANI nanoparticles, the reflection loss could only reach − 5.52 dB. When the loading of Fe_3O_4@PANI nanoparticles increases to 10.0 wt%, reflection loss can reach − 10.16 dB. However, for 30.0 wt% Fe_3O_4@PANI/epoxy nanocomposites, reflection loss even reaches − 35.9 dB, and the effective adsorption bandwidth is 2.24 GHz. Generally, as electromagnetic wave adsorption materials, the reflection loss should reach 10 dB at least. Hence, epoxy nanocomposites with 30.0 wt% Fe_3O_4@PANI nanoparticles can be applied for electromagnetic wave adsorption. In this work, with increasing Fe_3O_4@PANI nanoparticles, the reflection loss improved. This may be due to improved impedance matching, magnetic loss, and electrical loss caused by the introduction of magnetic and electrical conductive Fe_3O_4@PANI nanoparticles.

Figure 8(A) shows the DSC curves of the mixture of epoxy resin monomers and Fe_3O_4@PANI nanoparticles. It is obviously observed that there is a broad peak from 100–125 ^{o}C, which indicates chemical interaction between Fe_3O_4@PANI nanoparticles and epoxy resin monomers. Because there is no heat-releasing peak for only pure epoxy monomer and Fe_3O_4@PANI nanoparticles in the measured temperature range. In order to further confirm the chemical reaction. The FT-IR results of Fe_3O_4@PANI nanoparticles before and after reaction with epoxy resin monomers. For Fe_3O_4@PANI nanoparticles before reacting with epoxy resin monomers, Fig. 8B(a) shows all the characterized peaks of Fe3O4@PANI nanoparticles. However, for the Fe_3O_4@PANI nanoparticles after reacting with epoxy resin monomers, Fig. 8B(b), the peaks of Fe3O4@PANI nanoparticles are also observed. It is interesting to note that there is a peak located at around 1241 cm^{-1} within the marked region due to the strong absorption of C − O−C stretch vibration. Theoretically, the amine group on polyaniline could react with the epoxy group. Since after reacting with epoxy resin monomers and totally washing with acetone, the epoxy resin monomer should be removed. However, the observed new peak at 1241 cm^{-1} indicates the

interaction between polyaniline and epoxy [28]. Scheme 1 is the proposed interaction of the amine group on polyaniline with epoxy resin monomers.

4. Conclusion

In this work, the tensile strength of epoxy nanocomposites with Fe_3O_4@PANI is improved to 82.5 MPa. However, with high loading, the tensile strength decreased, which was induced by the agglomeration of Fe_3O_4@PANI. The improved thermal stability and glass transition temperature are observed in the TGA and DMA results. Moreover, the epoxy nanocomposites with high loading of Fe_3O_4@PANI nanoparticles show great potential for electromagnetic wav adsorption. The reflection loss even reaches 35.9 dB, with an effective adsorption bandwidth of 1.8 GHz. Moreover, the DSC and FT-IR results systematically studied the mechanism for the interaction between polyaniline and epoxy matrix. This work could provide the guideline for applying polyaniline as a coupling agent in epoxy composites with excellent electrical, magnetic and mechanical properties.

Declarations

Competing Interests:

The authors declare no competing interests.

Funding:

ZW would like to acknowledge the support from Oakland University.

Author Contribution

Hua Hou and Zhe Wang designed this project and contributed to the main manuscript text. Juanna Ren and Wenhao Dong conducted experiments. Ethan Burcar and Ashley DeMerle have contributed to conducting the experiments, preparing figures, and writing. All authors reviewed the manuscript.

Acknowledgement

ZW would like to acknowledge the support from Oakland University.

Data availability:

The authors declare that the data supporting the findings of this study are available within the paper. Should any raw data files be needed in another format, they are available from the corresponding author

upon reasonable request.

References

1. Zhu J et al (2010) In situ stabilized carbon nanofiber (CNF) reinforced epoxy nanocomposites. Journal of Materials Chemistry 20 4937–4948, https://doi.org/
2. Rahimian-Koloor SMR, Shokrieh MM (2023) Investigating the Effect of the Curing-induced Residual Stress on the Mechanical Behavior of Carbon Nanotube/Epoxy Nanocomposites by Molecular Dynamics Simulation. Eng Sci 22:817. https://doi.org/doi:10.30919/es8d817
3. Hiremath, A., Thipperudrappa , S. & Bhat, R.(2022) Surface Morphology Analysis using Atomic Force Microscopy and Statistical Method for Glass Fiber Reinforced Epoxy-Zinc Oxide Nanocomposites. Engineered Science 18 308-319, https://doi.org/ doi:10.30919/es8d702.
4. Li X et al (2023) Electrophoretically deposited rigid-flexible hybrid graphene oxide-polyethyleneimine on carbon fibers for synergistically reinforced epoxy nanocomposites. Adv Compos Hybrid Mater 6:152. https://doi.org/doi:10.1007/s42114-023-00726-0
5. Zhao M et al (2023) Stepwise assembling manganese dioxide nanosheets and metal-organic frameworks on carbon fiber for deriving desirable mechanical properties and flame retardancy of epoxy composites. Adv Compos Hybrid Mater 6:150. https://doi.org/doi:10.1007/s42114-023-00727-z
6. Pan D et al (2022) Vertically Aligned Silicon Carbide Nanowires/Boron Nitride Cellulose Aerogel Networks Enhanced Thermal Conductivity and Electromagnetic Absorbing of Epoxy Composites. Nano-Micro Lett 14:118. https://doi.org/doi:10.1007/s40820-022-00863-z
7. Zhu Q et al (2022) Hydrothermally synthesized ZnO-RGO-PPy for water-borne epoxy nanocomposite coating with anticorrosive reinforcement. Prog Org Coat. https://doi.org/10.1016/j.porgcoat.2022.107153. 172 107153, https://doi.org/doi:
8. Gu H et al (2013) Flame-Retardant Epoxy Resin Nanocomposites Reinforced with Polyaniline-Stabilized Silica Nanoparticles. Ind Eng Chem Res 52:7718–7728. https://doi.org/doi:10.1021/ie400275n
9. Gu H et al (2013) Epoxy resin nanosuspensions and reinforced nanocomposites from polyaniline stabilized multi-walled carbon nanotubes. J Mater Chem C 1:729–743. https://doi.org/doi:10.1039/C2TC00379A
10. Zhang Y et al (2018) Excellent corrosion protection performance of epoxy composite coatings filled with silane functionalized silicon nitride. J Polym Res. https://doi.org/doi:10.1007/s10965-018-1518-2. 25 130
11. Guo J et al (2024) Size effect of nanomagnetite on magnetoresistance of core-shell structured polyaniline nanocomposites. Adv Compos Hybrid Mater 7:62. https://doi.org/doi:10.1007/s42114-024-00868-9

12. Galarreta-Rodriguez I et al (2023) Magnetically activated 3D printable polylactic acid/polycaprolactone/magnetite composites for magnetic induction heating generation. Adv Compos Hybrid Mater 6:102. https://doi.org/doi:10.1007/s42114-023-00687-4
13. Wang X et al (2022) Fe3O4@PVP@DOX magnetic vortex hybrid nanostructures with magnetic-responsive heating and controlled drug delivery functions for precise medicine of cancers. Adv Compos Hybrid Mater 5:1786–1798. https://doi.org/doi:10.1007/s42114-022-00433-2
14. Lu J, Yang Y, Zhong Y, Hu Q, Qiu B (2022) The Study on Activated Carbon, Magnetite, Polyaniline and Polypyrrole Development of Methane Production Improvement from Wastewater Treatment. ES Food Agrofor 10:30–38. https://doi.org/doi:10.30919/esfaf802
15. Guo J et al (2017) Polypyrrole-interface-functionalized nano-magnetite epoxy nanocomposites as electromagnetic wave absorbers with enhanced flame retardancy. J Mater Chem C 5:5334–5344. https://doi.org/doi:10.1039/C7TC01502J
16. Gu H et al (2015) Strengthened Magnetoresistive Epoxy Nanocomposite Papers Derived from Synergistic Nanomagnetite-Carbon Nanofiber Nanohybrids. Adv Mater 27:6277–6282. https://doi.org/doi:https://doi.org/10.1002/adma.201501728
17. Wang B et al (2023) Magnetic surface molecularly imprinted polymers for efficient selective recognition and targeted separation of daidzein. Adv Compos Hybrid Mater 6:196. https://doi.org/doi:10.1007/s42114-023-00775-5
18. Zhou K et al (2023) Biomass porous carbon/polyethylene glycol shape-stable phase change composites for multi-source driven thermal energy conversion and storage. Adv Compos Hybrid Mater 6:34. https://doi.org/doi:10.1007/s42114-022-00620-1
19. Guo J et al (2016) Significantly enhanced mechanical and electrical properties of epoxy nanocomposites reinforced with low loading of polyaniline nanoparticles. RSC Adv 6:21187–21192. https://doi.org/doi:10.1039/C5RA25210E
20. Lu Q, Lu J, Sun D, Qiu B (2024) Fe3O4@PANI composite improves biotransformation of waste activated sludge into medium-chain fatty acid. Adv Compos Hybrid Mater 7:113. https://doi.org/doi:10.1007/s42114-024-00919-1
21. Zhu J et al (2010) Magnetic Epoxy Resin Nanocomposites Reinforced with Core – Shell Structured Fe@FeO Nanoparticles: Fabrication and Property Analysis. ACS Appl Mater Interfaces 2:2100–2107. https://doi.org/doi:10.1021/am100361h
22. Guo J et al (2014) Reinforced magnetic epoxy nanocomposites with conductive polypyrrole nanocoating on nanomagnetite as a coupling agent. RSC Adv 4:36560–36572. https://doi.org/doi:10.1039/C4RA07359B
23. Zhang X et al (2013) Strengthened magnetic epoxy nanocomposites with protruding nanoparticles on the graphene nanosheets. Polymer 54:3594–3604. https://doi.org/doi:https://doi.org/10.1016/j.polymer.2013.04.062
24. Zhang X et al (2015) Polypyrrole doped epoxy resin nanocomposites with enhanced mechanical properties and reduced flammability. J Mater Chem C 3:162–176.

https://doi.org/doi:10.1039/C4TC01978D

25. Wang H et al (2023) Research progress on electromagnetic wave absorption based on magnetic metal oxides and their composites. Adv Compos Hybrid Mater 6:120. https://doi.org/doi:10.1007/s42114-023-00694-5
26. Long Y et al (2023) Enhanced electromagnetic wave absorption performance of hematite@carbon nanotubes/polyacrylamide hydrogel composites with good flexibility and biocompatibility. Adv Compos Hybrid Mater 6:173. https://doi.org/doi:10.1007/s42114-023-00749-7
27. Lin J et al (2023) Ultralight, hierarchical metal–organic framework derivative/graphene hybrid aerogel for electromagnetic wave absorption. Adv Compos Hybrid Mater 6:177. https://doi.org/doi:10.1007/s42114-023-00762-w
28. Gu H et al (2012) Polyaniline Stabilized Magnetite Nanoparticle Reinforced Epoxy Nanocomposites. ACS Appl Mater Interfaces 4:5613–5624. https://doi.org/doi:10.1021/am301529t

Schemes

Scheme 1 is available in the Supplementary Files section.

Figures

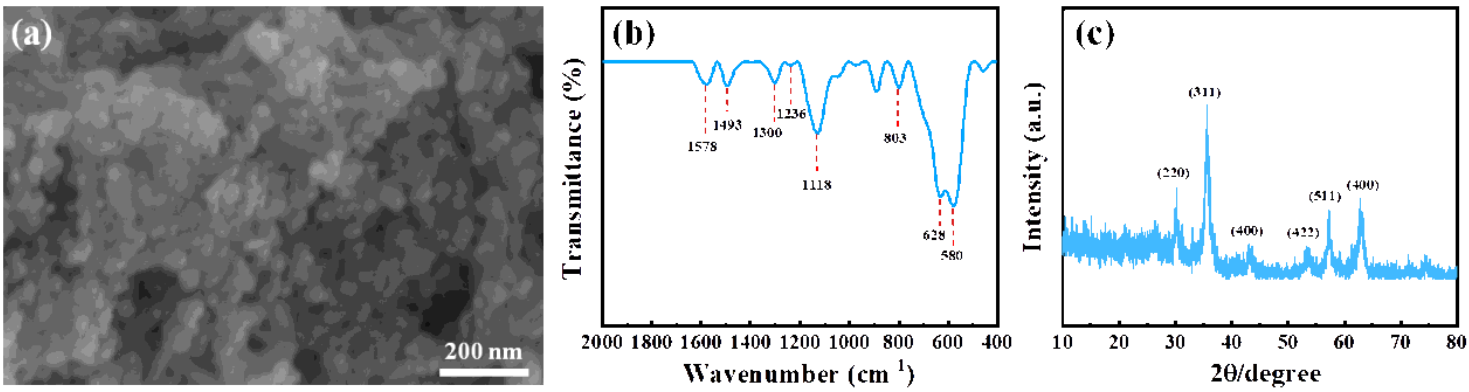

Figure 1

(a) SEM, (b) FT-IR and (c) XRD images for PANI@Fe_3O_4 particles.

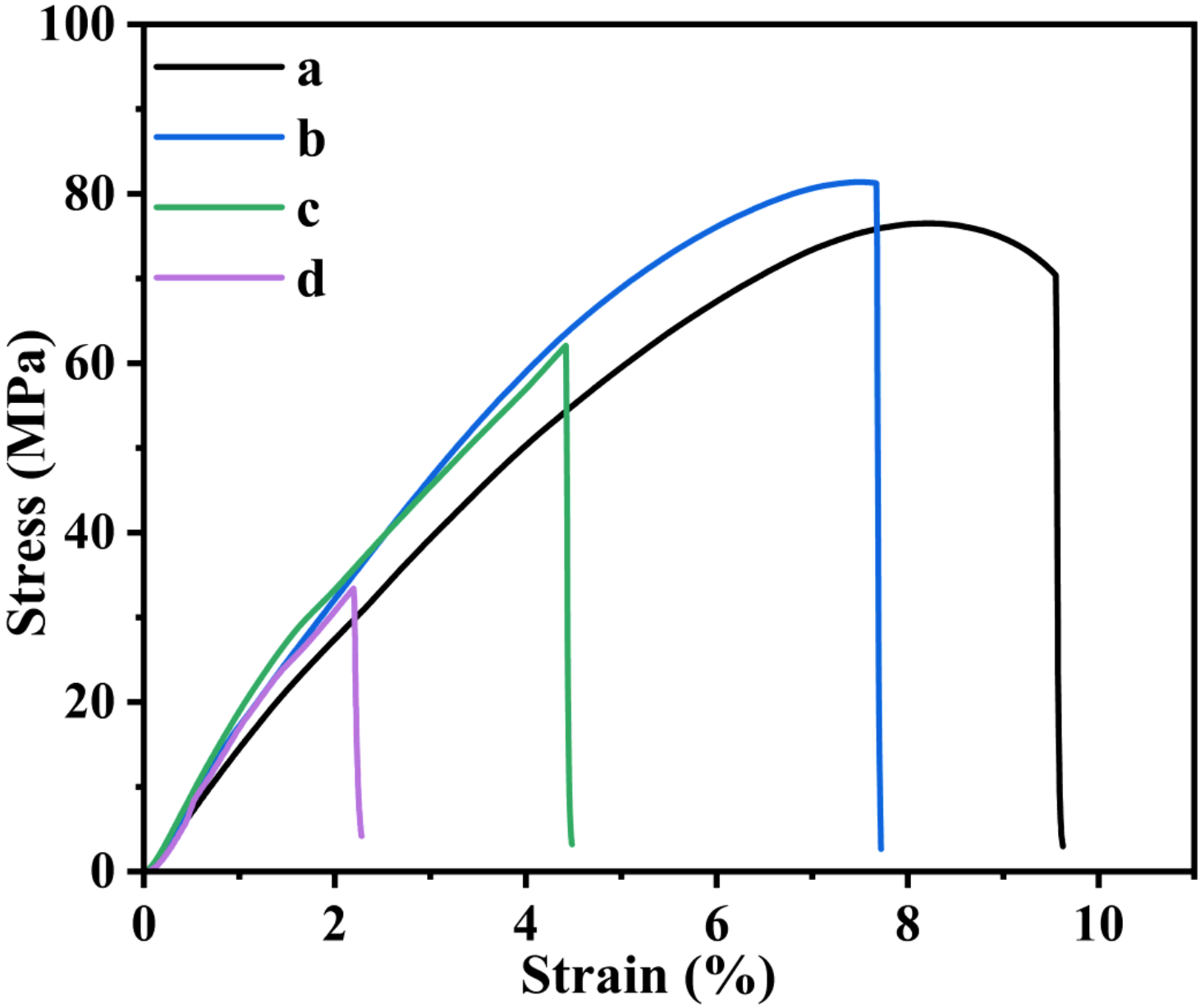

Figure 2

(A) stress-strain curves and (B) Young's modulus of (a) cured pure epoxy and epoxy nanocomposites with (b)1.0 , (c) 10.0 and (d) 30.0 wt% PANI@Fe_3O_4 nanoparticles.

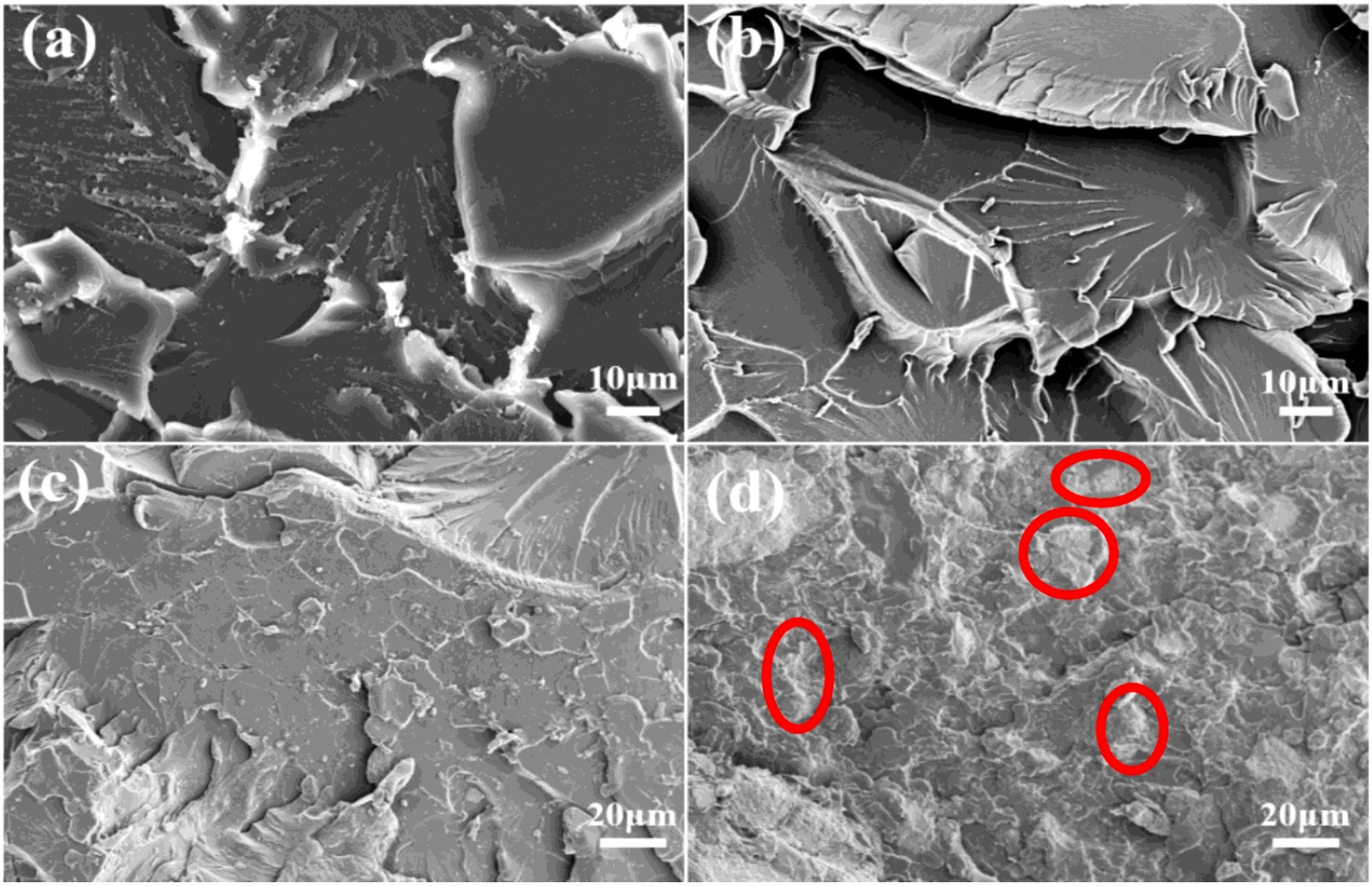

Figure 3

SEM microstructures of the fracture surface of (a) cured pure epoxy and its PNCs with (b) 1% Fe_3O_4@PANI /epoxy, (c) 10% Fe_3O_4@PANI /epoxy, and (d) 30% Fe_3O_4@PANI /epoxy.

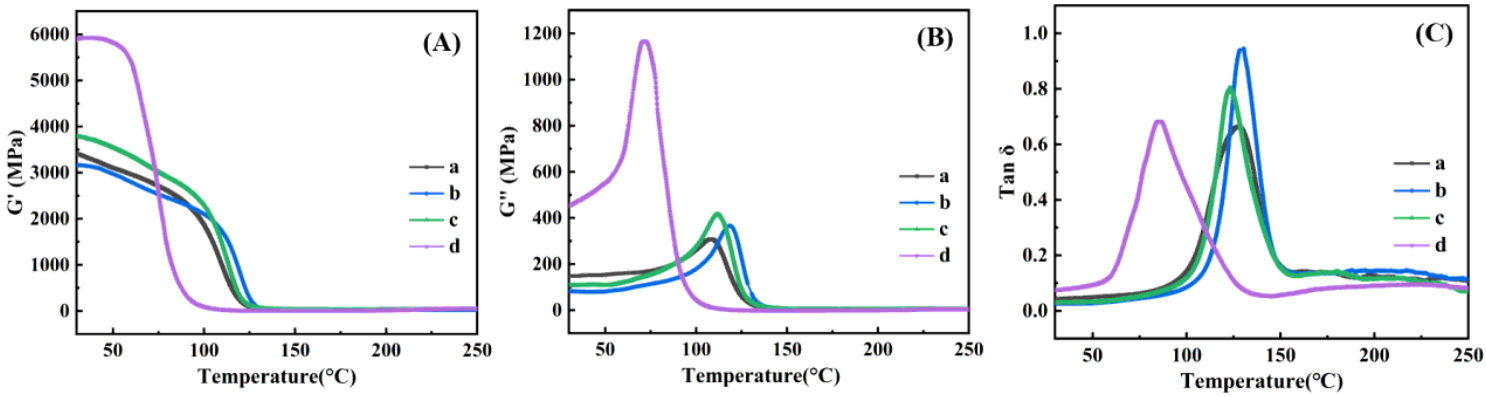

Figure 4

(A) storage modulus (G'), (B) loss modulus (G"), and (C) tanδ for (a) pure epoxy and epoxy nanocomposites with (b) 1%, (c) 10% and (d) 30% Fe_3O_4@PANI nanoparticles.

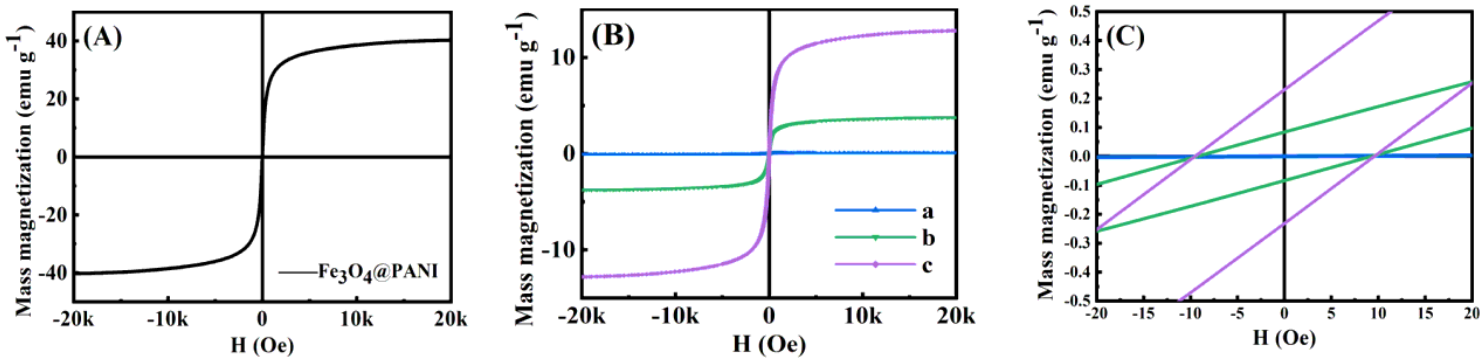

Figure 5

Room temperature magnetization curves of (A) Fe_3O_4@PANI nanoparticles, (B) epoxy nanocomposites with (a) 1%, (b) 10% and (c) 30% Fe_3O_4@PANI nanoparticles and area enlargement for epoxy nanocomposites.

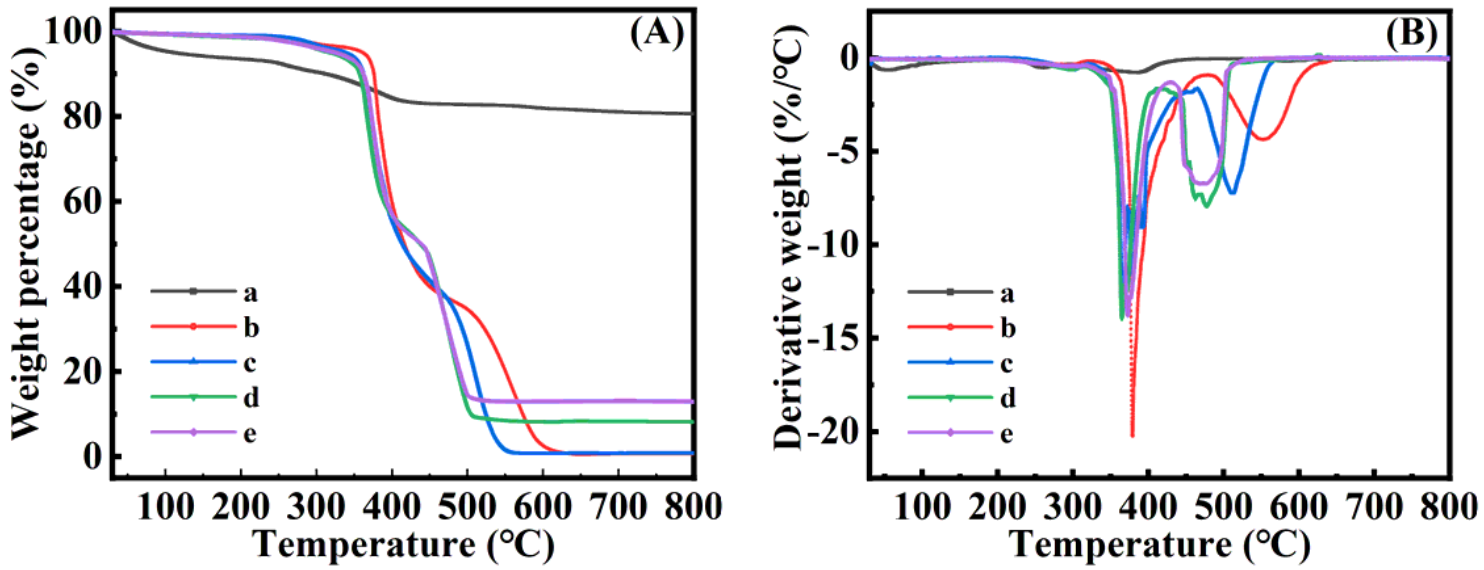

Figure 6

(A) TGA and (B) DTG curves of (a) Fe_3O_4@PANI nanoparticles, (b) pure epoxy and epoxy nanocomposites with (c) 1%, (d) 10% and (e) 30% Fe_3O_4@PANI nanoparticles.

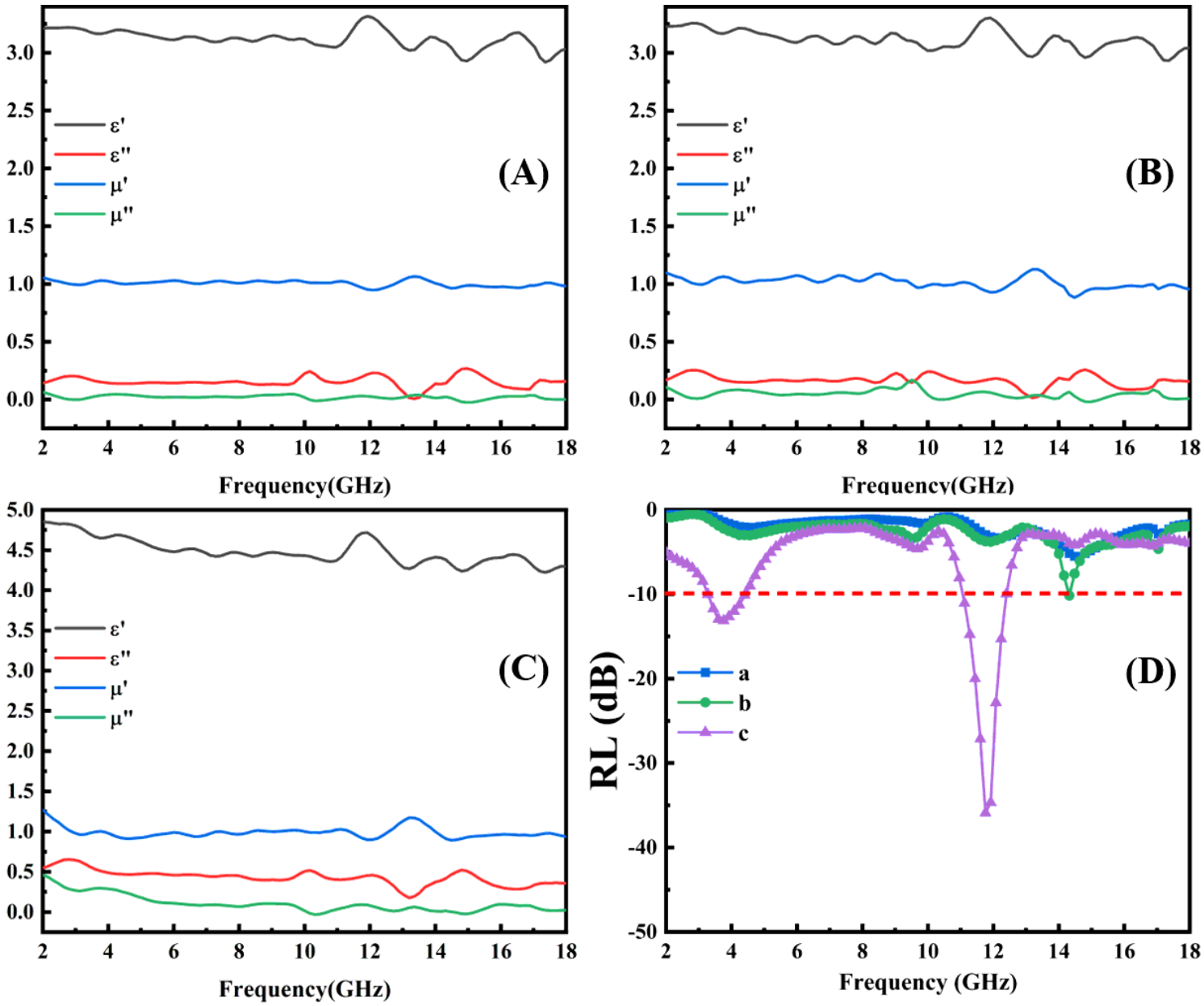

Figure 7

(A, B, C) permittivity and permeability as a function of frequency for epoxy nanocomposites with 1.0, 10.0 and 30.0 wt% of Fe_3O_4@PANI nanoparticles; (D) reflection loss as function of frequency for epoxy nanocomposites with (a)1.0, (b)10.0 and (c)30.0 wt% of Fe_3O_4@PANI nanoparticles.

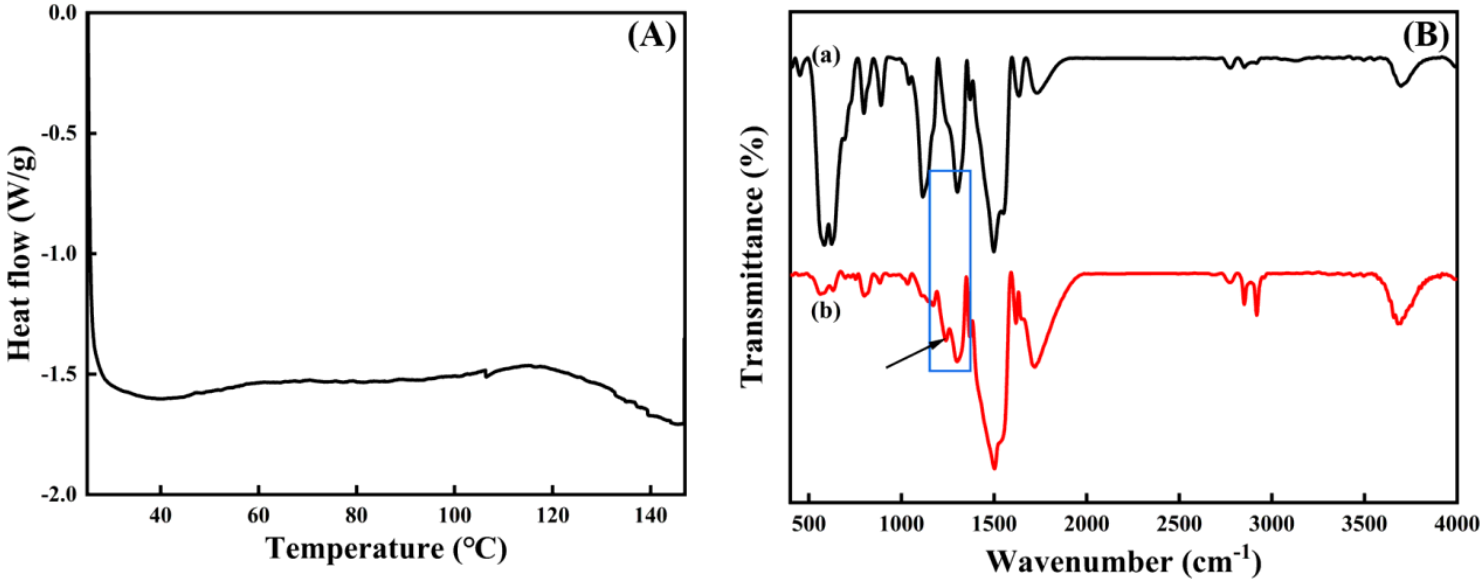

Figure 8

(A) DSC curve for epoxy resin monomers and Fe_3O_4@PANI nanoparticles; (B) FT-IR spectra of Fe_3O_4@PANI nanoparticles (a) before and (b) after reacted with epoxy resin monomers.

Supplementary Files

This is a list of supplementary files associated with this preprint. Click to download.

- Onlinefloatimage91.png
- Onlinefloatimage10.png
- 3.supportingmaterials.docx